Available online at www.sciencedirect.com

ScienceDirect

Sensors and Actuators B 130 (2008) 943–946

SENSORS AND ACTUATORS B CHEMICAL

www.elsevier.com/locate/snb

Short communication

A novel technique for measuring pico-scale flow rate of a liquid solution using a microchannel

Kow-Ming Chang *, Kuo-Yi Chao, Kun-Feng Lin

Department of Electronics Engineering Institute of Electronics, National Chiao Tung University, Hsinchu 30050, Taiwan

Received 16 February 2007; received in revised form 22 September 2007; accepted 10 October 2007
Available online 1 November 2007

Abstract

As micrototal analysis system (μ-TAS) becoming more extensively used, techniques for fabricating microchannels, microactuators, and measuring systems are becoming increasingly important. This study describes a novel method for fabricating a closed microchannel that can be used to measure the pico-scale flow rate of a liquid solution with an accuracy of better than 1 pL/s. The flow rate of 9 pL/s is calculated from the measurements. Without any high temperature or high-voltage processing, the microchannel can be integrated in the complementary metal–oxide–semiconductor (CMOS) microfluidic system and the fabricating process involves only some standard CMOS processes and common materials. The batch fabrication of a single integrated circuit (IC) chip is essential to reaching the goal of a system in one chip.

Keywords: Microchannel; Pico-liter; Sacrificial layer; Measuring; HDP-RIE

1. Introduction

Over the last decade, microchannels have become critical components of microfluidic systems, in which they have been used to connect between pumps, valves, and sensors [1]. Sometimes microchannels are employed to promote the miniaturization of such systems as electrophoresis [2–4], polymer chain reaction (PCR) [5,6], chromatography [7] and microreactor [8] systems. Glass-to-wafer or wafer-to-wafer bonding approaches are usually required to construct closed microchannels [9]. Several approaches to the bonding processes have been investigated. The most common bonding techniques are fusion bonding [10], anodic bonding [11], eutectic bonding [12], and adhesive bonding [13–15]. The main disadvantage of fusion bonding is the high-temperature annealing step (>800 °C) which may cause such problems as thermal stress, spreading of the doping profile, and instability of the IC components. Anodic bonding always proceeds at a very high voltage (>1200 V) that can damage other components. Metal contaminations and expensive materials are the main limitations of eutectic bonding. A polymer film is used as the intermediate bonding material in adhesive bonding such as BCB and PDMS. Adhesive bonding offers several advantages, such as low temperature, a low-cost process, and a simple spin on process. However, the potential disadvantages of adhesive bonding are limited long-term stability and difficulty with forming a hermetic seal. Also, sometimes some microvoids may be introduced during the bonding process that may affect the transfer rate of microchannels. If leakage of the liquid occurs, then other electronic components may be degraded. Buried microchannels (BCT) [16] in silicon can eliminate the need for aligned bonding, but the radius of the microchannels may not be very easy to control, since the process is time-controlled. Additionally, sealing the trench without any voids that could induce leaking is very difficult.

This investigation presents a novel method for creating a closed microchannel to solve the aforementioned problems of fabricating a microchannel and make it compatible with the IC processes. A high-density plasma reactive ion etching (HDP-RIE) system is adopted to etch bulk silicon and deposit a 5 μm thick silicon dioxide by plasma-enhanced chemical vapor deposition (PE-CVD) as a sacrificial layer. The cap-layer is PE-CVD nitride and the sacrificial layer is cleared in a buffered HF. After careful rinsing in the deionized water for 5 min and drying, sealing with sputtered Pt or Al is immediately performed.

* Corresponding author. Tel.: +886 935260072; fax: +886 3 5731887.
E-mail address: kmchang@cc.nctu.edu.tw (K.-M. Chang).

0925-4005/$ – see front matter © 2007 Elsevier B.V. All rights reserved.
doi:10.1016/j.snb.2007.10.047

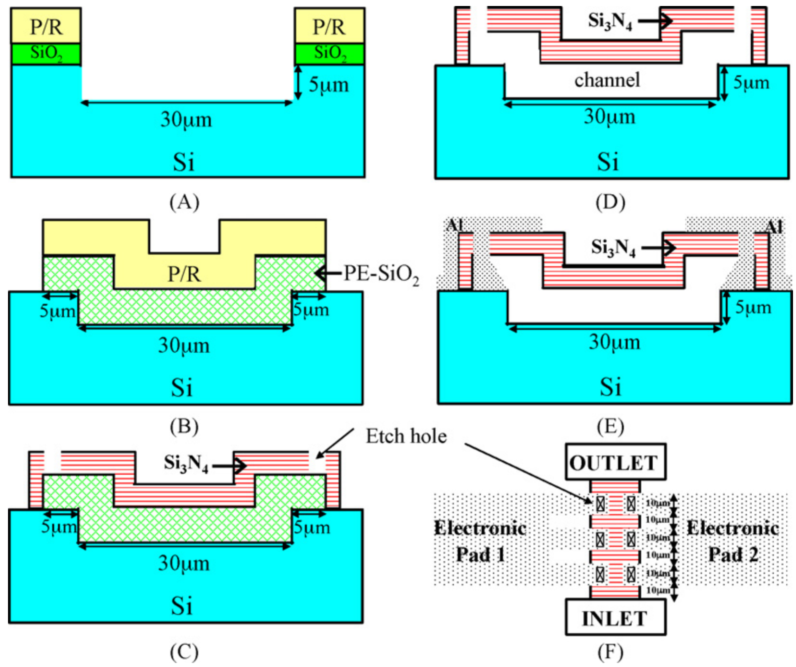

Fig. 1. Fabrication processes.

2. Fabrication

A microchannel was formed by surface silicon etching and sacrificial layers that were used in surface machined fabrication. This approach is more easily integrated into the IC processes than is bulk-machined fabrication. Fig. 1 presents the fabrication processes.

First, the RCA method was employed to clean 4 in. of bare silicon wafers. Then, a thermal silicon dioxide film was grown on both sides of the wafer by a furnace system at 1100 °C. Second, the microchannel and injection wells were defined by photo resist and etched by a HDP-RIE system, respectively. After the etching process, the substrate was rectangular with a width of 30 μm and a height of 5 μm (Fig. 1A). Third, a 5 μm thick silicon dioxide was deposited on the microchannel. A second pattern was defined and the silicon dioxide was etched by a HDP-RIE system that could yield a sharp sidewall (Fig. 1B). The sacrificial silicon dioxide was 40 μm wide, larger than the microchannel by 5 μm on both sides. The photo resist was cleared using a H_2SO_4 solution after the sacrificial layer had been patterned. Fourth, a 500-nm-thick layer of silicon nitride was formed on the top of the wafer using a PE-CVD system, following the use of a lithography process by mask III. The silicon nitride film was also etched using an HDP-RIE system. After the etching holes were etched on both sides of the microchannel (Fig. 1C), the sacrificial layer was cleared by BOE solution for 10 h (Fig. 1D) and rinsed in deionized water for 5 min. Finally, an aluminum electrode was sputtered onto the microchannels to fill up the etching holes. The measuring metal lines were patterned with the mask IV and etched using an aluminum etchant (Fig. 1E). Fig. 1F depicts the top view of this novel microchannel. It can be compared with Fig. 4. This method yielded minimum and maximum sizes of the microchannels of 5 μm in height and 5–100 μm in width in the experiment.

3. Results and discussion

Fig. 2 presents an SEM photograph of the cross-section of this microchannel. The microchannel was 30 μm wide and 5 μm high, and the pits in the bottom of microchannel were formed by the HDP-RIE system. However, these pits would be eliminated with a precise control of processing parameters. Fig. 3 presents a corner of microchannel. The etching holes were already perfectly stuffed. The aluminum electrodes had been patterned too. The most important thing for the novel microchannel is that if the etching holes have been stuffed up with aluminum film. Fig. 3 also indicates that the etching holes were already been uniformly

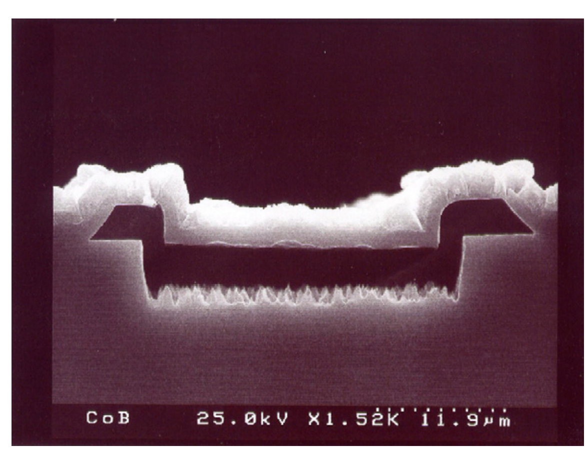

Fig. 2. An SEM photograph of the cross-section of this microchannel which was 30 μm wide and 5 μm high.

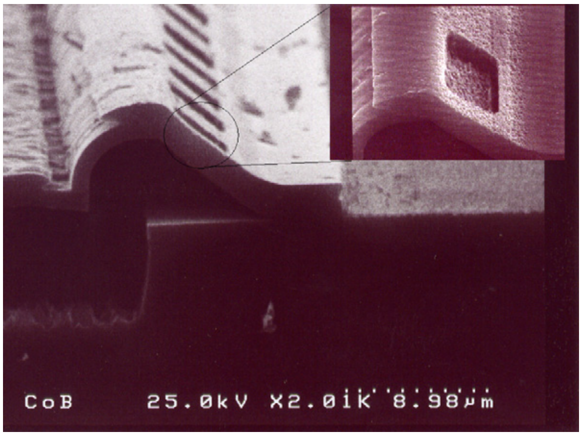

Fig. 3. The etching holes were already been uniformly filled with aluminum layer and no gap is observed.

filled with aluminum layer and no gap is observed. Using the closed microchannel with aluminum electrodes, a flow rate of several pL/s can be measured. A potassium chloride (KCl) aqueous solution with a conductivity of 0.24 S/cm was passed through the microchannel and the current between the two electrode pads was measured using an HP 4156A semiconductor parameter analyzer. Fig. 4 presents the top view of the novel measurement layout. The distance between etching holes is 10 μm and the cross-section area of the microchannel is 150 μm^2. Since the conductivity of two electrodes varies with time when the conductance solution passes through the novel microchannel, the current between two electronic pads can be measured to calculate the flow rate. The measurements of electronic characteristics are via the electronic pads which are in contact with metal tips. And the injection of liquid solution is via the inlet and outlet ports. The pipes connect the inlet and outlet ports using epoxy resins. The relationship between flow rate and measuring current is as follows:

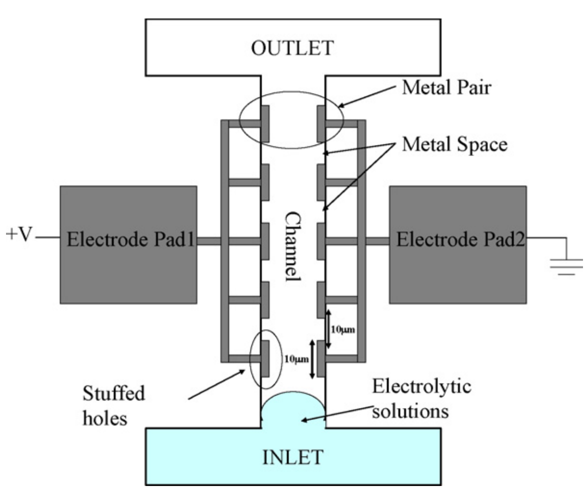

Fig. 4. The top view of the novel measurement layout. The distance between etching holes is 10 μm and the cross-section area of the microchannel is 150 μm^2.

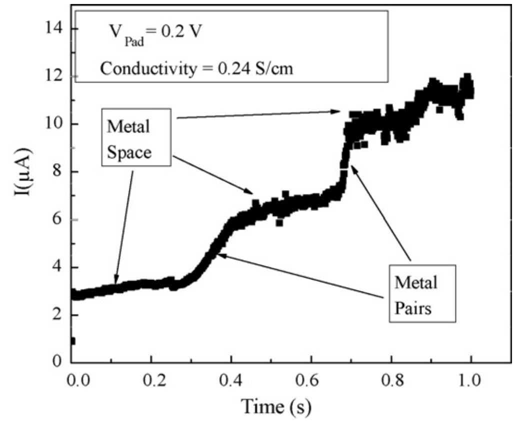

Fig. 5. The measurement of current stairs as time went by. Each current stair represents a pair of etching holes that are stuffed with aluminum. The measuring voltage is 0.2 V and the conductivity of the liquid solution is 0.24 S/cm. The flow rate of 9 pL/s is calculated from the measurements.

$$I = \frac{V}{R} = V \times \frac{1}{W/(\sigma \times l \times A/W)}$$
$$= V \times \frac{\sigma A l}{W^2} = CAl = Cv, \quad \text{where}$$
$$C = V \times \frac{\sigma}{W^2} = \text{constant} \quad \frac{\Delta I}{\Delta t} = \frac{\Delta v}{\Delta t} = \text{flow rate}$$

where I is the current between two pads, V is the voltages between two pads, R is the resistance between two pads, σ is the conductivity of liquid solution, W is the width of microchannel, A is the cross-section area of microchannel, l is the length of liquid solution, C is a constant number, v is the volume of liquid solution, and Δt is the total measuring time.

Fig. 5 plots the measurements made using an HP 4156A. Each current stair represents a pair of etching holes that are stuffed with aluminum. While the conductive solution is in contact with each metal pairs, the current increases linearly with time. When the conductive solution passes though the space between the metal pairs, the current is constant. Accordingly, with three stairs, as shown in Fig. 5, the liquid have already passed though the microchannel through a distance of 60 μm. The total passed volume is around 9 pL (6 × 10 μm × 5 μm × 30 μm) during 1 s. The flow rate of 9 pL/s is calculated from the measurements. The minimum volume that can be measured is about 1 pL for a microchannel with a length of 10 μm and an area of 150 μm^2. Therefore, the accuracy of the flow rate is about 1 pL/s. The novel microchannel enables a pico-scale flow rate of a liquid solution that is used in a nano-bio-system to be calculated precisely.

4. Conclusions

A novel microchannel was fabricated without any high-temperature or high-voltage process and aluminum was used uniformity to stuff the etching holes. The conductive method was employed to calibrate a pico-scale flow rate. The flow rate of 9 pL/s is calculated from the measurements. The accuracy of the microchannel is about 1 pL/s. When the size of the microchannels or the distance between the etching holes becomes small, the accuracy becomes extremely small.

Acknowledgement

The authors would like to thank the National Science Council of the Republic of China, Taiwan, for financially supporting this research under contract no. NSC-94-2215-E-009-012.

References

[1] S.C. Terry, J.H. Jerman, J.B. Angell, A gas chromatographic air analyzer fabricated on a silicon wafer, IEEE Trans. Electron Dev. 26 (1979) 1880–1886.
[2] J.R. Webster, C.H. Mastrangelo, Large-volume integrated capillary electrophoresis stage fabricated using micromachining of plastics on silicon substrates, in: Proceedings of the Transducers'97, Chicago, IL, June 16–19, 1997, pp. 503–506.
[3] H. Nakanishi, T. Nishimoto, N. Nakamura, S. Nagamachi, A. Arai, Y. Iwata, Y. Mito, Fabrication of electrophoresis devices on a quartz and glass substrates using a bonding with HF solution, in: Proceedings of the IEEE MEMS'97, Nagoya, Japan, January 26–30, 1997, pp. 299–304.
[4] H.F. Li, Z.W. Cai, J.M. Lin, Separation of catecholamines by microchip electrophoresis with a simple integrated laser-induced fluorescence detector, Anal. Chem. 565 (2006) 183–189.
[5] M. Albin, R. Kowallis, E. Picozza, Y. Raysberg, C. Sloan, E. Winn-Deen, T. Woudenber, J. Zupfer, Micromachining and microgenetics: what are they and where do they work together, in: Proceedings of the IEEE Solid-State Sensor and Actuator Workshop, Hilton Head'96, SC, June 2–6, 1996, pp. 253–257.
[6] J.A. Kim, J.Y. Lee, S. Seong, S.H. Cha, S.H. Lee, J.J. Kim, T.H. Park, Fabrication and characterization of a PDMS–glass hybrid continuous-flow PCR chip, J. Biochem. Eng. 29 (2006) 91–97.
[7] L.M. Pilarski, J. Lauzon, E. Strachan, S. Adamia, A. Atrazhev, A.R. Belch, C.J. Backhouse, Sensitive detection using microfluidics technology of single cell PCR products from high and low abundance IgH VDJ templates in multiple myeloma, J. Immunol. Methods 305 (2005) 94–105.
[8] R. Srinivasan, I.M. Hsing, P.E. Berger, K.F. Jensen, S.L. Firebaugh, M.A. Schmidt, M.P. Harold, J.J. Lerou, J.F. Ryley, Micromachined reactors for catalytic partial oxidation reactions, Am. Inst. Chem. Eng. J. 43 (11) (1997) 3059–3069.
[9] K. Schjolberg-Henriksen, E. Poppe, S. Moe, P. Storas, M.M.V. Taklo, D.T. Wang, H. Jakobsen, Anodic bonding of glass to aluminium, Microsyst. Technol. 12 (2006) 441–449.
[10] P.W. Barth, Silicon fusion bonding for fabrication of sensors, actuators, and microstructures, Sens. Actuator A21–A23 (1990) 919–926.
[11] H. Henmi, S. Shoji, Y. Shoji, K. Yoshimi, M. Esashi, Vacuum packaging for microsensors by glass–silicon anodic bonding, Sens. Actuator 43 (1994) 243–248.
[12] Y.T. Cheng, L. Lin, K. Najafi, Localized silicon fusion and eutectic bonding for MEMS fabrication and packaging, J. Microelectromech. Syst. 9 (1) (2000) 3–8.
[13] Y. Xia, G. Whitesides, Soft lithography, Angew. Chem. Int. Ed. 37 (1998) 550–575.
[14] B.H. Jo, L.M. Van Lerberghe, K.M. Motsegood, D.J. Beebe, Three-dimensional micro-channel fabrication in polydimethylsiloxane (PDMS) elastomer, J. Microelectromech. Syst. 9 (1) (2000) 76–81.
[15] W.W.Y. Chow, K.F. Lei, G. Shi, W.J. Li, Q. Huang, Microfluidic channel fabrication by PDMS-interface bonding, Smart Mater. Struct. 15 (2006) s112–s116.
[16] M.J. de Boer, R.W. Tjerkstra, J.W. (Erwin) Berenschot, H.V. Jansen, G.J. Burger, J.G.E. (Han) Gardeniers, M. Elwenspoek, A.V.D. Berg, Micromachining of buried micro channels in silicon, J. Microelectromech. Syst. 9 (1) (2000) 94–103.